Journal of Alloys and Compounds 526 (2012) 6–10

Contents lists available at SciVerse ScienceDirect

Journal of Alloys and Compounds

journal homepage: www.elsevier.com/locate/jallcom

Microstructures and hydrogen storage properties of $LaMg_{8.40}Ni_{2.34-x}Al_x$ alloys

Baozhong Liu[a,b], Jinhua Li[a], Shumin Han[a,c,*], Lin Hu[c], Lichao Pei[c], Mingzhi Wang[a]

[a] State Key Laboratory of Metastable Materials Science and Technology, Yanshan University, Qinhuangdao 066004, China
[b] School of Materials Science and Engineering, Henan Polytechnic University, Jiaozuo 454000, China
[c] College of Environmental and Chemical Engineering, Yanshan University, Qinhuangdao 066004, China

ARTICLE INFO

Article history:
Received 6 October 2011
Received in revised form 13 February 2012
Accepted 13 February 2012
Available online xxx

Keywords:
Hydrogen storage
La–Mg–Ni alloy
Thermodynamics
Kinetics

ABSTRACT

Herein, we prepared a new type of magnesium and transition metal-based alloys with the formula of $LaMg_{8.40}Ni_{2.34-x}Al_x$ ($x = 0$ and 0.20). Their phase structures, morphologies and hydrogen storage properties were studied by different methods. The XRD patterns show that $LaMg_{8.40}Ni_{2.34-x}Al_x$ alloys are made of La_2Mg_{17}, $LaMg_2Ni$ and Mg_2Ni phases. The SEM images indicate that the phase distributions in $LaMg_{8.40}Ni_{2.14}Al_{0.20}$ alloy are more uniform compared with $LaMg_{8.40}Ni_{2.34}$ alloy. In addition, the reversible hydrogen storage capacity of $LaMg_{8.40}Ni_{2.14}Al_{0.20}$ alloy is 3.22 wt.% at 558 K, which is higher than that of $LaMg_{8.40}Ni_{2.34}$ alloy. The partial substitution of Al for Ni effectively improves the hydrogen storage capacity, as well as the hydriding/dehydriding kinetics of the alloys, with the evidence that 89% hydrogen in the saturated state in $LaMg_{8.40}Ni_{2.14}Al_{0.20}$ alloy was released in 1500 s at 573 K, while only 74% hydrogen in the saturated state in $LaMg_{8.40}Ni_{2.34}$ alloy was released at the same conditions. Consequently, we believe that the alloying of aluminum in the magnesium-rare earth-transition metal-based alloys can effectively improve their hydrogen storage performance.

1. Introduction

Magnesium and magnesium-based alloys are attractive candidate materials for reversible hydrogen storage due to their high hydrogen storage capacity, outstanding reversibility and low cost [1]. However, their slow hydriding/dehydriding kinetics as well as the highly thermodynamic stability of their corresponding hydrides slow down the rhythms of Mg-based alloys for practical applications [2,3]. Many attempts have been made to improve the hydrogen storage performance of Mg-based alloys, such as chemical doping [4,5], addition of catalyst [6,7], mechanical alloying [8,9], melt spinning [10,11] and GPa hydrogen pressure method [12]. The refinement of alloy microstructures down to nanometer-sized grains by mechanical alloying or melt spinning obviously enhanced the hydrogen storage performance. However, both mechanical alloying and melt spinning need extensive precautions to keep the materials pure and dense to minimize the oxidation and fire risk [13]. Consequently, alloying with some simple and low-cost methods such as inducing melting is a more practical method to improve the hydrogen storage properties.

Generally, the alloying of rare earth (RE) elements or transition metal is effective to improve the hydrogen storage properties of Mg [14–16]. One reason is that the RE hydrides can form during the first hydrogen absorption process and catalyze the hydrogen absorption and desorption reactions in the alloys, therefore improve the hydriding/dehydriding kinetics of Mg hydride. Recently, the alloying of transition metals, such as Ti, Mn, Ni, Co, V, Cu, have been demonstrated to be effective in destabilizing the Mg hydride and enhancing the hydriding/dehydriding kinetics [17–19]. Furthermore, people have reported that $LaMg_2Cu$ alloy with $LaMg_2Cu_2$ and $LaMg_3$ phases and $LaMg_2Ni_{1.67}$ alloy with La_2Mg_{17}, $LaMg_3$ and Mg_2Ni phases can exhibit excellent adsorption and desorption kinetics with the explanation of abundant phase interfaces as hydrogen diffusion channels and buffer areas for the release of distortion and stress of the crystal lattice in the alloys [20,21]. Therefore, it is believed that the multiphase RE-Mg-Ni alloys should exhibit outstanding hydrogen storage properties.

Later on, further investigation revealed that Al hydride can exhibit even higher hydrogen storage capacity compared with Mg hydride, with both the theoretical and experimental evidences that the alloying of Al can decrease the decomposition enthalpy of the alloys [22,23]. Thus, it can be expected that the hydrogen storage properties will be further improved by partially alloying of Al in La–Mg–Ni alloys. Our previous research has demonstrated that $LaMg_{8.40}Ni_{2.34}$ alloy with multiphase structures can exhibit fast hydriding/dehydriding kinetics [24]. Herein, we studied the influence of Al on the microstructures and hydrogen storage properties of the $LaMg_{8.40}Ni_{2.34-x}Al_x$ ($x = 0$ and 0.20).

* Corresponding author. Tel.: +86 335 807 4648; fax: +86 335 807 4648.
E-mail address: hanshm@ysu.edu.cn (S. Han).

0925-8388/$ – see front matter © 2012 Elsevier B.V. All rights reserved.
doi:10.1016/j.jallcom.2012.02.085

2. Experimental procedures

$LaMg_{8.40}Ni_{2.34-x}Al_x$ ($x = 0$ and 0.20) alloy ingots were prepared by melting La, Mg, Ni and Al (purity more than 99.9%) in an alumina crucible under argon atmosphere. After melting, the alloys were annealed at 723 K for 10 h under argon atmospheres with the pressure of 0.08 MPa. The phase structures of the alloys were studied by D/max-2500/PC X-ray diffractometer with Cu Kα radiation. The SEM specimens were mechanically smoothed and then polished under the distilled water. The phase composition images were obtained by using HITACHI S-4800 scanning electron microscope (SEM) with an energy dispersive X-ray spectrometer (EDS). The average element composition was calculated based on five different spots. The hydrogen storage properties of the alloys were studied by using pressure-composition-temperature (PCT) (made by Suzuki Shokan in Japan). To calculate the enthalpy and entropy, hydrogen pressure at midpoint of the absorption pressure plateau of PCT curves was taken. In the PCT measurement, the delay time was 300 s and the maximum pressure was 3 MPa. The hydriding/dehydriding kinetics of the alloy were tested with the initial hydrogen pressure of 5 MPa and 0.01 MPa, respectively.

3. Results and discussion

3.1. Phase structures and morphologies of $LaMg_{8.40}Ni_{2.34-x}Al_x$ alloys

Fig. 1 shows the XRD patterns of $LaMg_{8.40}Ni_{2.34-x}Al_x$ alloy as well as the simulated XRD pattern of $LaMg_2Ni$ which is calculated based on the cell parameters and the atom positions of the single crystal $LaMg_2Ni$ [25]. It can be seen that $LaMg_{8.40}Ni_{2.34-x}Al_x$ alloys are made of La_2Mg_{17}, $LaMg_2Ni$ and Mg_2Ni phases. Fig. 2a shows the SEM image of $LaMg_{8.40}Ni_{2.34}$ alloy with different color distribution, including dark grey areas (A, La_2Mg_{17}), white areas (B, $LaMg_2Ni$) and light grey areas (C, Mg_2Ni), indicating the phase distribution in $LaMg_{8.40}Ni_{2.34}$ alloy is not uniform. As a comparison, the SEM image of $LaMg_{8.40}Ni_{2.14}Al_{0.20}$ alloy (Fig. 2b) shows continuous dark grey areas (D, La_2Mg_{17}), dispersive white areas (E, $LaMg_2Ni$) and separated grey dots (F, Mg_2Ni), which clearly demonstrates that the phase distribution of $LaMg_{8.40}Ni_{2.14}Al_{0.20}$ alloy is more uniform than that of $LaMg_{8.40}Ni_{2.34}$ alloy. In addition, according to the EDS results listed in Table 1, Al element can only be observed in the La_2Mg_{17} phase, not in the $LaMg_2Ni$ or Mg_2Ni phase.

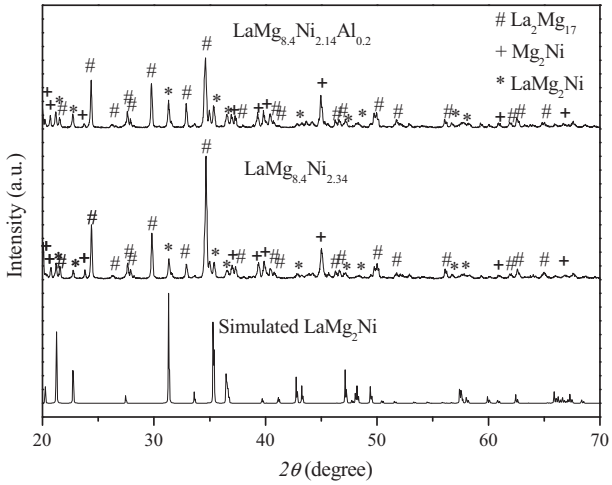

Fig. 1. XRD patterns of $LaMg_{8.40}Ni_{2.34-x}Al_x$ alloys and simulated XRD patterns of $LaMg_2Ni$.

3.2. Hydrogen storage properties of $LaMg_{8.40}Ni_{2.34-x}Al_x$ alloys

The hydrogen storage property of $LaMg_{8.40}Ni_{2.34-x}Al_x$ alloys was analyzed by using PCT at different temperatures. Before the measurement, $LaMg_{8.40}Ni_{2.34-x}Al_x$ alloys were activated with initial

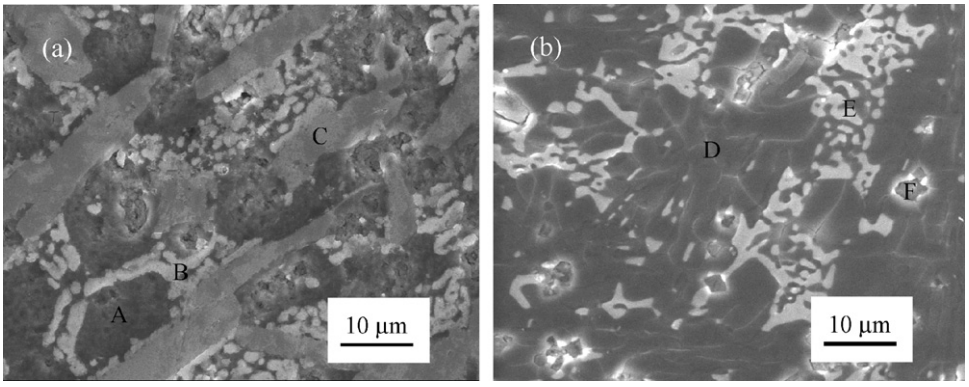

Fig. 2. SEM images of $LaMg_{8.40}Ni_{2.34-x}Al_x$ alloys; (a) $x = 0$ and (b) $x = 0.20$.

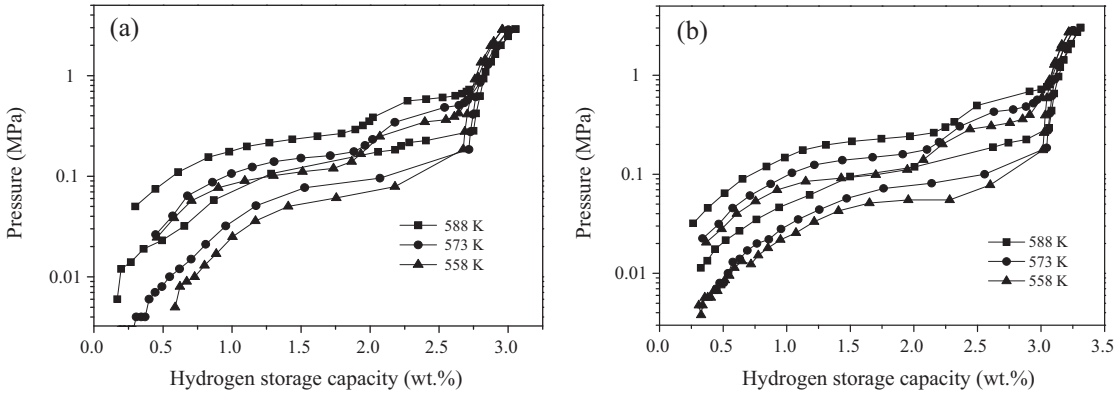

Fig. 3. PCT curves of $LaMg_{8.40}Ni_{2.34-x}Al_x$ alloys at different temperatures; (a) $x = 0$ and (b) $x = 0.20$.

Table 1
Results of EDS analysis for $LaMg_{8.40}Ni_{2.34-x}Al_x$ alloys.

Element	$LaMg_{8.4}Ni_{2.34}$ alloy						$LaMg_{8.4}Ni_{2.14}Al_{0.20}$ alloy					
	Mg_2Ni		$LaMg_2Ni$		La_2Mg_{17}		Mg_2Ni		$LaMg_2Ni$		La_2Mg_{17}	
	w (%)	*x* (%)	*w* (%)	*x* (%)	*w* (%)	*x* (%)	*w* (%)	*x* (%)	*w* (%)	*x* (%)	*w* (%)	*x* (%)
Mg	43.94	66.21	21.38	52.98	49.93	80.89	44.47	66.90	27.43	61.19	42.53	76.95
Ni	52.75	32.92	22.10	22.64	12.68	8.51	50.64	31.55	19.63	18.14	9.09	6.82
La	3.31	0.81	56.52	24.47	37.79	10.60	5.89	1.55	52.92	20.67	47.73	15.13
Al											0.68	1.10

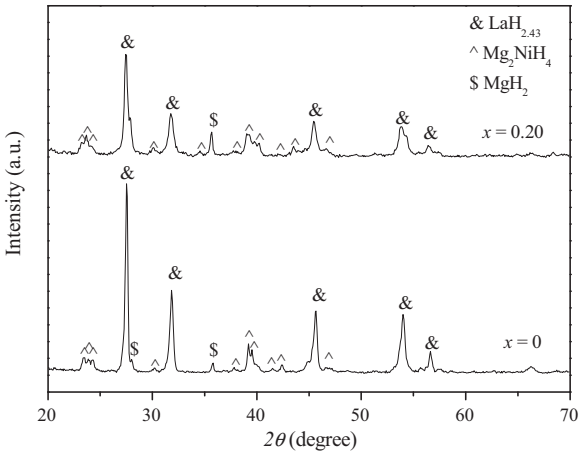

Fig. 4. XRD patterns of $LaMg_{8.40}Ni_{2.34-x}Al_x$ alloys after first hydrogen absorption.

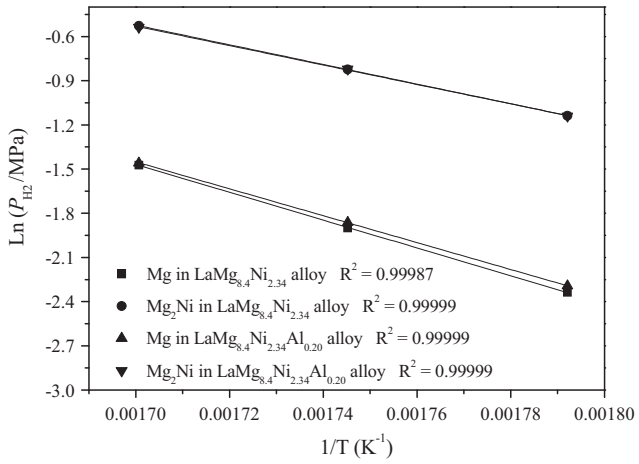

Fig. 5. Van't Hoff plots of hydriding Mg and Mg_2Ni in $LaMg_{8.40}Ni_{2.34-x}Al_x$ alloys.

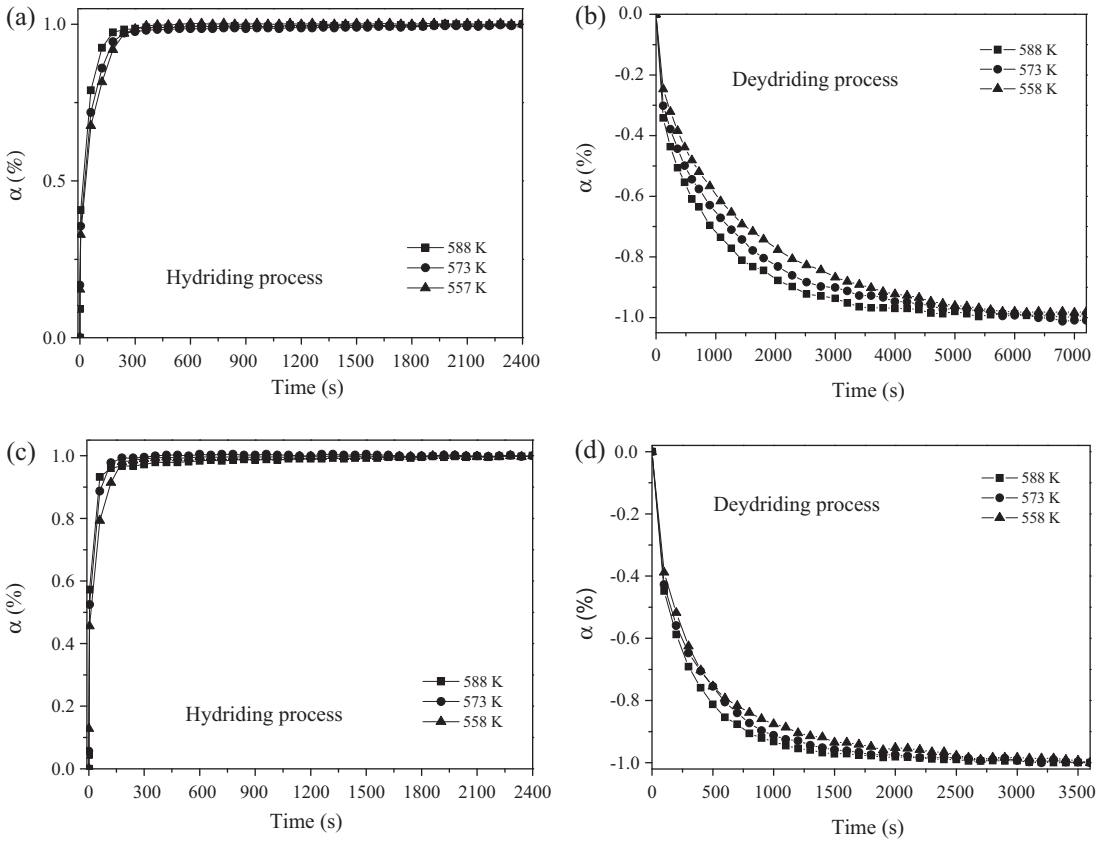

Fig. 6. Hydriding and dehydriding curves of $LaMg_{8.40}Ni_{2.34-x}Al_x$ alloys at different temperatures; (a), (b) $x = 0$ and (c), (d) $x = 0.20$.

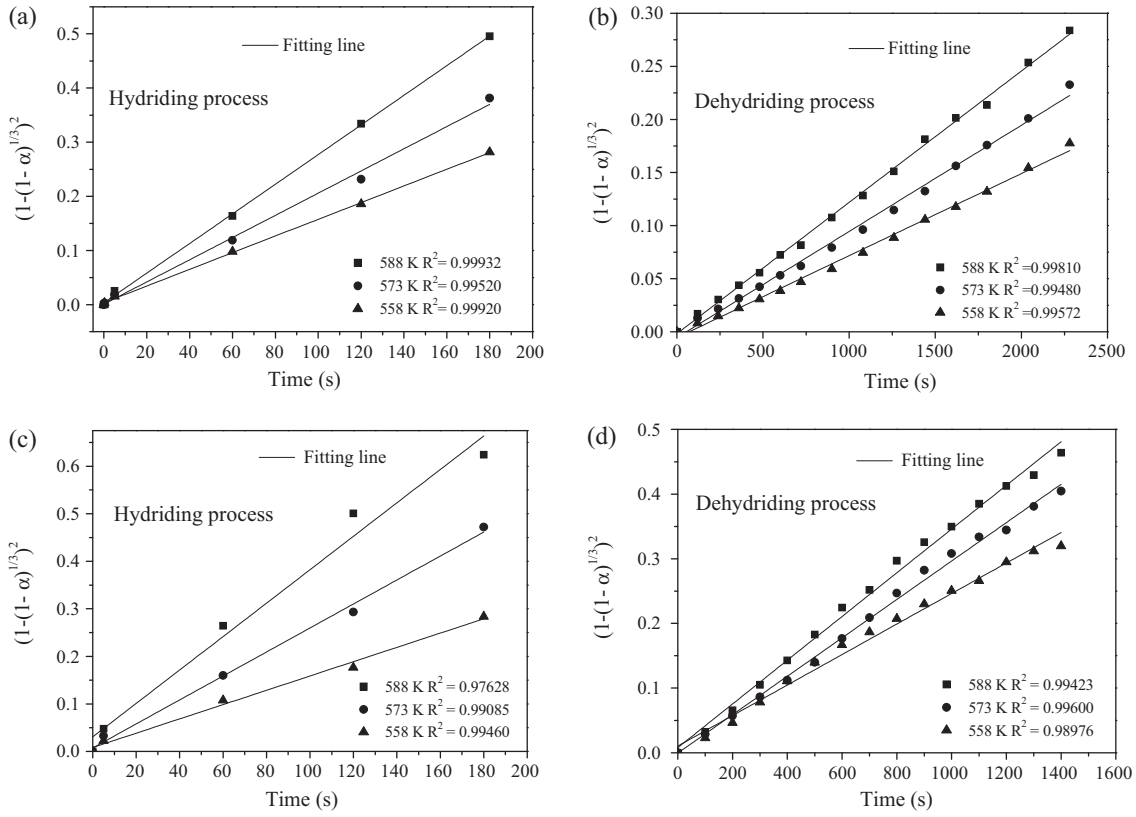

Fig. 7. Plots of $(1-(1-\alpha)^{1/3})^2$ vs. t for hydriding and dehydriding processes of $LaMg_{8.40}Ni_{2.34-x}Al_x$ alloys; (a), (b) $x = 0$ and (c), (d) $x = 0.20$.

hydrogen pressure of 5 MPa at 588 K. Fig. 3 shows the PCT curves of $LaMg_{8.40}Ni_{2.34-x}Al_x$ alloys at 558 K, 573 K and 588 K, respectively. At 558 K, the reversible hydrogen storage capacities of $LaMg_{8.40}Ni_{2.34}$ and $LaMg_{8.40}Ni_{2.14}Al_{0.20}$ alloys are 3.01 wt.% and 3.22 wt.%, respectively. The higher hydrogen capacity of $LaMg_{8.40}Ni_{2.14}Al_{0.20}$ alloy can be ascribed to the following factors. Firstly, the alloying of Al can effectively boost the dehydrogenation process, thus increase the hydrogen storage capacity of Mg-based alloys [23,24]. Secondly, Al atoms are lighter than Ni atoms, which is favorable to increase the hydrogen capacity of the alloys per unit mass. In addition, both the alloys exhibit two pressure plateaus, indicating that two different hydrides were formed in the hydriding process. After the first hydrogen absorption, the XRD patterns of $LaMg_{8.40}Ni_{2.34-x}Al_x$ alloys (588 K, initial pressure of 5 MPa) shown in Fig. 4 indicates that both $LaMg_{8.40}Ni_{2.34}$ and $LaMg_{8.40}Ni_{2.14}Al_{0.20}$ alloys are made of the $LaH_{2.43}$, Mg_2NiH_4 and MgH_2 phases without any observed peak of the La_2Mg_{17} or $LaMg_2Ni$ phases. That can be ascribed to the reactions of La_2Mg_{17} and $LaMg_2Ni$ phases with hydrogen. Detailed discussions of the phase transformation during the activation process of $LaMg_{8.40}Ni_{2.34}$ alloy can be found in our previous report [22]. Because the hydrogen storage capacity of La hydride is limited [16], Mg_2Ni and Mg have been the main hydrogen storage phases in the following hydrogen absorption and desorption cycles. Thus, it is believed that the plateau in the hydriding curves at the lower pressure is corresponding to the formation of MgH_2 and the other plateau at the higher pressure is corresponding to the formation of Mg_2NiH_4. However, only one pressure plateau appears in the dehydriding curves of the two alloys, which is due to the simultaneous reactions of both MgH_2 and Mg_2NiH_4 in the dehydriding process. Since the desorption pressure of Mg_2NiH_4 is higher than that of MgH_2 at the same temperature, Mg_2NiH_4 should first desorbs hydrogen and exhibit a significant volume contraction, thereby resulting a significant contraction strain of MgH_2.In addition, the dehydrogenation of Mg_2NiH_4 can be slightly inhibited due to the stabilization by MgH_2 [26,27].

To obtain the thermodynamic parameters of the hydriding reactions of Mg and Mg_2Ni in $LaMg_{8.40}Ni_{2.34-x}Al_x$ alloys, the plateau pressure and the temperature were correlated based on the Van't Hoff equation, which is shown in Fig. 5. The enthalpy and entropy of hydriding Mg in $LaMg_{8.40}Ni_{2.34}$ alloy are -76.0 ± 0.6 kJ/mol and -116 ± 2.4 J/mol/K, respectively, and those of hydriding Mg_2Ni in $LaMg_{8.40}Ni_{2.34}$ alloy are -54.9 ± 0.1 kJ/mol and -88.9 ± 1.1 J/mol/K, respectively. For, the enthalpy and entropy in the reaction of hydriding Mg in $LaMg_{8.40}Ni_{2.14}Al_{0.20}$ alloy are -73.4 ± 0.3 kJ/mol and -111 ± 1.3 J/mol/K, respectively, and those in the reaction of hydriding Mg_2Ni in the $LaMg_{8.40}Ni_{2.14}Al_{0.20}$ alloy are -54.3 ± 0.3 kJ/mol and -87.9 ± 1.2 J/mol/K, respectively. Based on those data, we believe that the Mg hydride in $LaMg_{8.40}Ni_{2.14}Al_{0.20}$ alloy is less stable than that in $LaMg_{8.40}Ni_{2.34}$ alloy, whereas the stability of Mg_2Ni hydride in two alloys is similar. As mentioned above, Al element can be observed in the La_2Mg_{17} phase of $LaMg_{8.40}Ni_{2.14}Al_{0.20}$ alloy. Furthermore, La_2Mg_{17} phase can be transferred to $LaH_{2.43}$ and Mg hydride in the first hydrogen absorption. Therefore, it is believed that Al atoms can partially solute in the Mg hydride of the $LaMg_{8.40}Ni_{2.14}Al_{0.20}$ alloy and make the Mg hydride in $LaMg_{8.40}Ni_{2.14}Al_{0.20}$ alloy less stable. However, the stability of the Mg_2Ni hydride in the two alloys is close to each other because Al element cannot be found in the $LaMg_2Ni$ and Mg_2Ni phases in $LaMg_{8.40}Ni_{2.14}Al_{0.20}$ alloy, as well as the $LaMg_2Ni$ and Mg_2Ni phases can be transferred to the Mg_2Ni hydride in the activation process.

Hydrogen sorption kinetic properties of $LaMg_{8.40}Ni_{2.34-x}Al_x$ alloys were studied independently at 558 K, 573 K and 588 K. Hydrogen sorption curves of two alloys are shown in Fig. 6. The hydrogen in the two alloys reached 99% of the saturated value in less than 450 s. In the dehydriding process, 89% hydrogen of

the saturated state in $LaMg_{8.40}Ni_{2.14}Al_{0.20}$ alloy can be released in 1500 s at 573 K. In comparison, only 74% hydrogen of the saturated state in $LaMg_{8.40}Ni_{2.34}$ alloy can be released under the same condition, which indicates that the dehydriding performance of $LaMg_{8.40}Ni_{2.14}Al_{0.20}$ alloy is better than that of $LaMg_{8.40}Ni_{2.34}$ alloy.

The sorption reaction mechanisms of two alloys were analyzed by fitting the observed hydriding/dehydriding rate curves with the rate equation derived from the two different processes [28,29]. The hydriding and dehydriding curves of two alloys at different temperatures can be fitted by using Jander diffusion model with the equation of $(1-(1-\alpha)^{1/3})^2 = kt$ (Fig. 7). The activation energy (E_a) values of two alloys in the hydriding and dehydriding processes can be obtained based on the methods described by Hu et al. [21] and Li et al. [29]. The E_a values in the hydriding process of $LaMg_{8.40}Ni_{2.34}$ and $LaMg_{8.40}Ni_{2.14}Al_{0.20}$ alloys are 52.4 ± 0.4 kJ/mol and 50.3 ± 0.1 kJ/mol, respectively. The E_a values in the dehydriding process of $LaMg_{8.40}Ni_{2.34}$ and $LaMg_{8.40}Ni_{2.14}Al_{0.20}$ alloys are 59.2 ± 0.1 kJ/mol and 57.3 ± 0.2 kJ/mol, respectively. Those results further confirm that the sorption performance of $LaMg_{8.40}Ni_{2.14}Al_{0.20}$ alloy is better than that of $LaMg_{8.40}Ni_{2.34}$ alloy. The major reason can be explained by more uniform phase distributions in $LaMg_{8.40}Ni_{2.14}Al_{0.20}$ alloy. RE hydride can catalyze the hydrogen desorption of Mg hydride and Mg_2Ni hydride [15,16]. Furthermore, Mg_2Ni are useful in the dehydriding process of Mg hydride [30]. Thus, the size, shape and distribution of RE hydride, Mg_2Ni hydride and Mg hydride will affect the catalytic performance in hydriding/dehydriding process. In our studies, La_2Mg_{17}, $LaMg_2Ni$ and Mg_2Ni phases can be transferred to La hydride, Mg hydride and Mg_2Ni hydride in the first hydrogen absorption. It is reasonable to assume that La, Mg and Ni atoms cannot diffuse into the surroundings during the activation process because of the relatively low temperature (588 K). In other words, the distribution of La hydride, Mg hydride and Mg_2Ni hydride is determined by the phase distribution of the alloys. As shown in Fig. 2, the phase distribution of $LaMg_{8.40}Ni_{2.14}Al_{0.20}$ alloy is more uniform than that of $LaMg_{8.40}Ni_{2.34}$ alloy. Therefore, RE hydride and Mg_2Ni phase in $LaMg_{8.40}Ni_{2.14}Al_{0.20}$ alloy can exhibit better catalytic effect during the hydrogen sorption process than that in $LaMg_{8.40}Ni_{2.34}$ alloy.

4. Conclusions

The $LaMg_{8.40}Ni_{2.34-x}Al_x$ ($x = 0, 0.20$) alloys have the same phase compositions of La_2Mg_{17}, $LaMg_2Ni$ and Mg_2Ni. However, their phase morphologies are obviously different. The phase distribution of $LaMg_{8.40}Ni_{2.14}Al_{0.20}$ alloy is more uniform compared with that of $LaMg_{8.40}Ni_{2.34}$ alloy. The PCT curves show that the reversible hydrogen storage capacity of $LaMg_{8.40}Ni_{2.14}Al_{0.20}$ is higher at 558 K, with the value of 3.22 wt.% versus 3.01 wt.% of $LaMg_{8.40}Ni_{2.34}$. According to the calculations, the Mg hydride in $LaMg_{8.40}Ni_{2.14}Al_{0.20}$ alloy is less stable than that in $LaMg_{8.40}Ni_{2.34}$ alloy, which should be attributed to the fact that Mg hydride is transformed from the reaction of La_2Mg_{17} with hydrogen in the activation process and the Al element can solute in the La_2Mg_{17} phase. In addition, $LaMg_{8.40}Ni_{2.14}Al_{0.20}$ alloy also shows faster hydriding and dehydriding kinetics. Therefore, we believe the partial substitution of Al for Ni can effectively enlarge the hydrogen storage capacity and improve the kinetic performance of magnesium and transition metal-based alloys, which will definitely boost the development of high hydrogen storage alloys.

Acknowledgments

This research is financially supported by the Hi-Tech Research and the Development Program of China (2007AA05Z117), the National Natural Science Foundation of China (50971112, 51001043), the China Postdoctoral Science Foundation funded project (20100470990) and the Natural Science Foundation of Hebei Province of China (E2010001170).

References

[1] J. Lu, Y.J. Choi, Z.Z. Fang, H.Y. Sohn, E. Ronnebro, J. Am. Chem. Soc. 131 (2009) 15843–15852.
[2] M. Anik, F. Karanfil, N. Küçükdeveci, Int. J. Hydrogen Energy 37 (2012) 299–308.
[3] Y.H. Cho, A.K. Dahle, J. Alloys Compd. 509S (2011) S621–S624.
[4] H.C. Zhong, H. Wang, L.Z. Ouyang, M. Zhu, J. Alloys Compd. 509 (2011) 4268–4272.
[5] Y. Zhang, B. Li, H. Ren, X. Ding, X. Liu, L. Chen, J. Alloys Compd. 509 (2011) 2808–2814.
[6] I.E. Malka, J. Bystrzycki, T. Płociński, T. Czujko, J. Alloys Compd. 509S (2011) S616–S620.
[7] Y. Zhu, Y. Yang, L. Wei, Z. Zhao, L. Li, J. Alloys Compd. (2012), doi:10.1016/j.jallcom.2012.01.018.
[8] A.A.C. Asselli, D.R. Leiva, A.M. Jorge Jr., T.T. Ishikawa, W.J. Botta, J. Alloys Compd. (2012), doi:10.1016/j.jallcom.2011.12.103.
[9] H. Shao, M. Felderhoff, F. Schüth, Int. J. Hydrogen Energy 36 (2011) 10828–10833.
[10] Y. Zhang, F. Hu, Z. Li, K. Lü, S. Guo, X. Wang, J. Alloys Compd. 509 (2011) 294–300.
[11] D. Guzmán, S. Ordoñez, J.F. Fernández, C. Sánchez, D. Serafini, P.A. Rojas, C. Aguilar, P. Tapia, Mater. Charact. 62 (2011) 442–450.
[12] X. Yang, N. Takeichi, K. Shida, H. Tanaka, N. Kuriyama, T. Sakai, J. Alloys Compd. 509 (2011) 1211–1216.
[13] M. Krystian, M.J. Zehetbauer, H. Kropik, B. Mingler, G. Krexner, J. Alloys Compd. 509S (2011) S449–S455.
[14] S. Kalinichenka, L. Röntzsch, T. Riedl, T. Weigärber, B. Kieback, Int. J. Hydrogen Energy 36 (2011) 10808–10815.
[15] H.J. Lin, L.Z. Ouyang, H. Wang, J.W. Liu, M. Zhu, Int. J. Hydrogen Energy 37 (2012) 1145–1150.
[16] A.A. Poletaev, R.V. Denys, J.K. Solberg, B.P. Tarasov, V.A. Yartys, J. Alloys Compd. 509S (2011) S633–S639.
[17] Q. Zheng, Y. Pivak, L.P.A. Mooij, A.M.J. van der Eerden, H. Schreuders, P.E. de Jongh, J.H. Bitter, B. Dam, Int. J. Hydrogen Energy (2012), doi:10.1016/j.ijhydene.2011.11.107.
[18] T. Liu, T. Zhang, C. Qin, M. Zhu, X. Li, J. Power Sources 196 (2011) 9599–9604.
[19] S. Tao, P.H.L. Notten, R.A. van Santen, A.P.J. Jansen, J. Alloys Compd. 509 (2011) 210–216.
[20] H. Ren, Y. Zhang, B. Li, D. Zhao, S. Guo, X. Wang, Int. J. Hydrogen Energy 34 (2009) 1429–1436.
[21] L. Hu, S. Han, J. Li, C. Yang, Y. Li, M. Wang, Mater. Sci. Eng. B 166 (2010) 209–212.
[22] J. Zhang, Y.N. Huang, C. Mao, P. Peng, Y.M. Shao, D.W. Zhou, Int. J. Hydrogen Energy 22 (2011) 14477–14483.
[23] A. Glage, R. Ceccato, I. Lonardelli, F. Girardi, F. Agresti, G. Principi, S. Gialanell, J. Alloys Compd. 478 (2009) 273–280.
[24] J. Li, B. Liu, S. Han, L. Hu, X. Zhu, M. Wang, Acta Phys.-Chim. Sin. 27 (2011) 403–407.
[25] M.D. Chio, A. Ziggiotti, G. Baricco, Intermetallics 16 (2008) 102–106.
[26] A. Zaluska, L. Zaluski, J.O. Ström-Olsen, J. Alloys Compd. 289 (1999) 197–206.
[27] H. Blomqvist, E. Rönnebro, D. Noréus, T. Kuji, J. Alloys Compd. 330–332 (2002) 270–286.
[28] Q. Li, K.C. Chou, Q. Lin, L.J. Jiang, F. Zhan, Int. J. Hydrogen Energy 29 (2004) 843–849.
[29] Q. Li, K.C. Chou, Q. Lin, L.J. Jiang, F. Zhan, Int. J. Hydrogen Energy 29 (2004) 1383–1388.
[30] S. Kalinichenka, L. Rontzsch, B. Kieback, Int. J. Hydrogen Energy 34 (2009) 7749–7755.